QCD TESTS FROM TAU-DECAY DATA

A. Pich

Departament de Física Teórica and Institut de Física Corpuscular, (CSIC), Universitat de València, 46100 Burjassot, Spain

ABSTRACT

The semileptonic tau-decay provides useful information on the algebra of currents of QCD. It is shown how good experimental data on the decay modes of the tau lepton, can be used for testing fundamental aspects of the strong interactions (chiral symmetry, resonance structures, vacuum condensates, $\Lambda_{\overline{MS}}$,...).

1. INTRODUCTION

Besides its intrinsic interest as a sequential lepton in the standard model of electroweak interactions, the tau is the only presently known lepton heavy enough to decay into hadrons. Therefore, its semileptonic decays appear to be an ideal laboratory for studying the hadronic weak currents in very clean conditions. Contrary to the well known $e^+e^- \longrightarrow \gamma^* \longrightarrow$ hadrons process, which only tests the electromagnetic vector current, the semileptonic tau-decay modes offer the possibility to study the properties of both vector and axial currents.

Within the standard model the τ lepton decays via the W-emission diagram shown in figure 1. Since the W coupling to the charged current is of universal

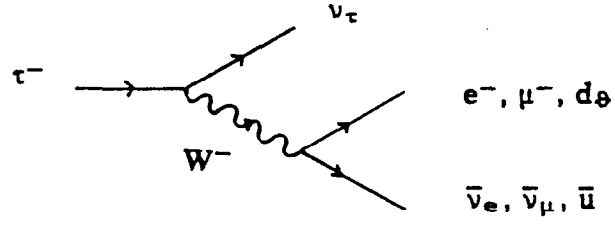

Fig.1. Feynman diagram for the decay of the τ lepton.

strength,

$$L_{cc} = \frac{g}{2\sqrt{2}} W_\mu^+ \left\{ \sum_l \bar{\nu}_l \gamma^\mu (1-\gamma_5) l + \bar{u} \gamma^\mu (1-\gamma_5) d_\theta \right\} + \text{h.c.} \ , \qquad (1.1)$$

there are five equal contributions (if final masses and gluonic corrections are neglected) to the τ^- decay width. Two of them correspond to the decay modes $\nu_\tau e^- \bar{\nu}_e$ and $\nu_\tau \mu \bar{\nu}_\mu$, while the other three are associated with the three possible colours of the quark-antiquark pair in the final $\nu_\tau d_\vartheta \bar{u}$ mode ($d_\vartheta \equiv \cos\vartheta_c d + \sin\vartheta_c s$). Hence, the branching fractions for the different channels are expected to be approximately,

$$\text{Br}\,(\tau^- \to \nu_\tau l^- \bar{\nu}_l) \sim \frac{1}{5} = 20\%\,, \quad (l=e,\mu)$$

$$R_H \equiv \frac{\Gamma(\tau^- \to \nu_\tau + \text{hadrons})}{\Gamma(\tau^- \to \nu_\tau e^- \bar{\nu}_e)} \simeq N_c = 3, \tag{1.2}$$

which should be compared with the formal*) experimental averages [1]

$$\text{Br}\,(\tau^- \to \nu_\tau e^- \bar{\nu}_e) = (17.5 \pm 0.4)\%$$

$$\text{Br}\,(\tau^- \to \nu_\tau \mu^- \bar{\nu}_\mu) = (17.8 \pm 0.4)\%$$

$$R_H = (3.54 \pm 0.08)\%\,. \tag{1.3}$$

The agreement if fairly good. Notice that the measured tau hadronic width provides strong evidence for the colour degree of freedom. We will discuss later whether the QCD dynamics is able to explain the difference between the measured value of R_H and the lowest order prediction $R_H = N_c$.

The tau-decay partial width for the leptonic modes $\tau \to \nu_\tau l \bar{\nu}_l$ ($l = e, \mu$) is easily computed, with the result (neutrinos are assumed to be massless)

$$\Gamma(\tau^- \to \nu_\tau l^- \bar{\nu}_l) = \frac{G_F^2 m_\tau^5}{192\pi^3} f(m_l^2/m_\tau^2) r\,, \tag{1.4}$$

where $f(x) = 1 - 8x + 8x^3 - x^4 - 12x^2 \ln x$. The factor r takes into account radiative corrections not included in the Fermi coupling constant G_F, and the non-local structure of the W-propagator. It has been estimated [2] to be $r = 0.9960$.

Eq. (1.4) gives a relation between the tau lifetime and the electronic branching ratio,

$$\text{Br}\,(\tau^- \to \nu_\tau e^- \bar{\nu}_e) = \tau_\tau / (1.600\, 10^{-12}\,\text{sec}). \tag{1.5}$$

Using the world average measured τ-lifetime [1], $\tau_\tau = (3.04 \pm 0.09)\, 10^{-13}$ sec, one gets the prediction

$$\text{Br}\,(\tau^- \to \nu_\tau e^- \bar{\nu}_e)_{th} = (19.0 \pm 0.6)\%\,, \tag{1.6}$$

which is about two standard deviations higher than the measured branching fraction of $(17.5 \pm 0.4)\%$. Given the present limit [3] of $m_{\nu_\tau} < 35$ MeV (95% C.L.), this small discrepancy cannot be due to a non-zero value of the tau neutrino mass.

The agreement is slightly better in the muonic channel. Taking into account the phase space mass correction, $f(m_\mu^2/m_\tau^2) = 0.9728$, one predicts

*) The number quoted for R_H results from averaging three different values which slightly disagree. See section five for details.

$$Br(\tau^- \to \nu_\tau \mu^- \bar{\nu}_\mu)_{th} = (18.5 \pm 0.6)\%, \tag{1.7}$$

which compares reasonably well with the measured value of $(17.8 \pm 0.4)\%$. Note, however, that in both cases the experimental branching fractions are below the values extracted theoretically from the measured lifetime.

The semileptonic decay modes of the tau, $\tau^- \to \nu_\tau H^-$, probe the matrix element of the left-handed charged current between the vacuum and the final hadronic state H^-,

$$<H^-|\bar{d}_\vartheta \gamma^\mu (1-\gamma_5) u|0>. \tag{1.8}$$

For the decay modes with lowest multiplicity, $\tau^- \to \nu_\tau \pi^-$ and $\tau^- \to \nu_\tau K^-$, the relevant matrix elements are already known from the measured decays $\pi^- \to \mu^- \bar{\nu}_\mu$ and $K^- \to \mu^- \bar{\nu}_\mu$. The corresponding τ-decay widths can then be predicted rather accurately. Including the computed electroweak radiative corrections[2], one gets

$$\frac{\Gamma(\tau^- \to \nu_\tau \pi^-)}{\Gamma(\tau^- \to \nu_\tau e^- \bar{\nu}_e)} = 0.601 \qquad \frac{\Gamma(\tau^- \to \nu_\tau K^-)}{\Gamma(\tau^- \to \nu_\tau e^- \bar{\nu}_e)} = 0.0399. \tag{1.9}$$

These numbers are in good agreement with the experimental ratios, which are measured to be (0.617 ± 0.037) and (0.038 ± 0.011) respectively[1].

In the Cabibbo allowed modes with $J^P = 1^-$, the matrix element of the vector charged current can also be obtained, through an isospin rotation, from the isovector part of the e^+e^- annihilation cross-section into hadrons, which measures the hadronic matrix element of the I=1 component of the electromagnetic current,

$$<H^0|(\bar{u}\gamma^\mu u - \bar{d}\gamma^\mu d)|0> . \tag{1.10}$$

The tau-decay width for these modes is then expressed as an integral over the corresponding e^+e^- cross-section[4],

$$\frac{\Gamma(\tau^- \to \nu_\tau V^-)}{\Gamma(\tau^- \to \nu_\tau e^- \bar{\nu}_e)} = \frac{3\cos^2\vartheta_c}{2\pi\alpha^2 m_\tau^8} \int_0^{m_\tau^2} ds\,(m_\tau^2 - s)^2 (m_\tau^2 + 2s)\, s\, \sigma^{I=1}_{e^+e^- \to V^0}(s). \tag{1.11}$$

Electroweak radiative corrections have been estimated[2] to increase this result by 2.36%. Taking this into account, the available $e^+e^- \to 2\pi$, 4π data imply[5]

$$\frac{\Gamma(\tau^- \to \nu_\tau \pi^- \pi^0)}{\Gamma(\tau^- \to \nu_\tau e^- \bar{\nu}_e)} = 1.26 \qquad [\text{exp.: } 1.27 \pm 0.07]$$

$$\frac{\Gamma(\tau^- \to \nu_\tau 2\pi^- \pi^+ \pi^0)}{\Gamma(\tau^- \to \nu_\tau e^- \bar{\nu}_e)} = 0.281 \qquad [\text{exp.: } 0.25 \pm 0.09] \tag{1.12}$$

$$\frac{\Gamma(\tau^- \to \nu_\tau \pi^- 3\pi^0)}{\Gamma(\tau^- \to \nu_\tau e^- \bar{\nu}_e)} = 0.056 \qquad [\text{exp.: } 0.17 \pm 0.15],$$

where the measured experimental ratios[1] are given inside brackets for comparison. The predictions agree quite well with the data. Note, however, that the extraction of the isovector part from the measured e^+e^- cross section requires model dependent assumptions (e.g. ρ-ω interference has to be taken into

account) and moreover, there is an additional systematic error due to the overall normalization of the e^+e^- annihilation cross section.

The exclusive tau-decays into final hadronic states with $J^P = 1^+$, or Cabibbo suppressed modes with $J^P = 1^-$ cannot be predicted with the same degree of confidence . We can only make model-dependent estimates with an accuracy which depends on our ability to handle the strong interactions at low energies. However, that just indicates that the decay of the tau lepton is providing us new experimental hadronic information . Due to their semileptonic character, the hadronic tau-decay data can be then a unique and extremely useful tool to learn about the couplings of the low-lying mesons to the weak currents. In the following, I will try to give a few examples to show how tau-decay data can be used for testing different aspects of strong interaction phenomena.

2. EXCLUSIVE SEMILEPTONIC DECAYS

At low momentum transfer, the coupling of a state H of n pseudoscalar mesons to the V-A current can be estimated in a very easy way by using the effective chiral realization of QCD, which, to lowest order in derivatives and masses, is given by ($f_\pi = 93.3$ MeV)[6]

$$L_{strong} \simeq \frac{1}{4} f_\pi^2 \mathrm{Tr}\left(\partial_\mu U \partial^\mu U^+\right) + \upsilon\, \mathrm{Tr}\left(MU + U^+ M\right) . \qquad (2.1)$$

The 3×3 special unitary matrix $U \equiv \exp(i\sqrt{2}\,\Phi/f_\pi)$ incorporates the octet of pseudoscalar mesons, which appear as Goldstone coordinate fields $\vec{\varphi}(x)$,

$$\Phi(x) \equiv \frac{\vec{\lambda}}{\sqrt{2}}\,\vec{\varphi}(x) = \begin{pmatrix} \frac{\pi^0}{\sqrt{2}} + \frac{\eta}{\sqrt{6}} & \pi^+ & K^+ \\ \pi^- & -\frac{\pi^0}{\sqrt{2}} + \frac{\eta}{\sqrt{6}} & K^0 \\ K^- & \bar{K}^0 & -\frac{2}{\sqrt{6}}\eta \end{pmatrix} \quad ; \qquad (2.2)$$

M denotes the diagonal quark mass matrix, M=diag (m_u, m_d, m_s), and

$$\upsilon = \frac{f_\pi^2\, m_{\pi^+}^2}{2(m_u+m_d)} = \frac{f_\pi^2\, m_{K^+}^2}{2(m_u+m_s)} = \frac{f_\pi^2\, m_{K^0}^2}{2(m_d+m_s)} . \qquad (2.3)$$

In this realization, the vector and axial currents are given by

$$\begin{aligned} V_\mu &= i(\Phi \overleftrightarrow{\partial_\mu} \Phi) + O(\Phi^4) \\ &\quad - \frac{iN_c}{6\sqrt{2}\,\pi^2 f_\pi^3}\,\varepsilon_{\mu\nu\alpha\beta}\left[\partial^\nu\Phi\;\partial^\alpha\Phi\;\partial^\beta\Phi + O(\Phi^5)\right] \\ A_\mu &= \sqrt{2}\, f_\pi\, \partial_\mu\Phi - \frac{\sqrt{2}}{3 f_\pi}\left[\Phi, (\Phi \overleftrightarrow{\partial_\mu} \Phi)\right] + O(\Phi^5) \\ &\quad - \frac{N_c}{12\pi^2 f_\pi^4}\,\varepsilon_{\mu\nu\alpha\beta}\left[\partial^\nu\Phi\;\partial^\alpha\Phi\;(\Phi \overleftrightarrow{\partial^\beta} \Phi) + O(\Phi^6)\right] , \end{aligned} \qquad (2.4)$$

where the odd-parity pieces, proportional to the Levi-Civita pseudotensor, come from the Wess-Zumino-Witten term of the chiral lagrangian[7], which takes into account the non-abelian chiral anomaly of QCD.

Tau decays involve, however, high values of momentum transfer, where the formulae given above no longer apply. Nevertheless we can still construct a reasonable model, taking into account the low energy theorems contained in the chiral realization. The amplitudes

$$T_\mu(p_1,\ldots,p_n) \equiv \langle H \left| (V-A)_\mu \exp\left(i\int d^4z\, L_{strong}(z)\right)\right| 0\rangle \qquad (2.5)$$

obtained from eqs. (2.1)-(2.4) must be continued from threshold by suitable final state interaction enhancements, which take into account the possible resonance structures present in each channel in a phenomenological way[8,9]. This can be done by weighting the contribution of a given set of pseudoscalars, with definite quantum numbers, with the appropriate resonance form factor. The requirement that the chiral predictions must be recovered below the resonance region, fixes the normalization of these form factors to be one at zero invariant mass. I take the standard ansatz

$$F_R(s) = \frac{M_R^2}{M_R^2 - s - iM_R\Gamma_R(s)}\ , \qquad (2.6)$$

where $M_R(\Gamma_R)$ denotes the mass (width) of the resonance R.

Let's try to apply this model to the decay $\tau^- \to \nu_\tau\, \pi^+\pi^-\pi^-$, which is expected to be dominated by the $J^P = 1^+ a_1(1260)$ (before $A_1(1270)$) resonance. This mode has been measured in recent years by four different experiments which have extracted the mass and width resonance parameters from a fit to the total invariant mass distribution of the three pions. The published results are shown in table 1. For comparison I have included the Data Particle Group values for the a_1-parameters, before (86) and after (88) the tau-decay measurements.

Table 1

	$B_r(\tau^- \to \nu_\tau \pi^+\pi^-\pi^-)$ (%)	M_{a_1}(MeV)	Γ_{a_1}(MeV)
DELCO[10]	5.0 ± 1.0	1056 ± 30	476 ± 140
MARK II[11]	7.8 ± 0.9	1194 ± 20	462 ± 70
ARGUS[12]	5.6 ± 0.7	1046 ± 11	521 ± 27
MAC[13]	7.8 ± 0.8	1166 ± 21	405 ± 79
PDG '86[14]	8.1 ± 0.7	1275 ± 28	316 ± 45
PDG '88[1]	6.8 ± 0.6	1260 ± 30	300 - 600

The measured three pion effective mass spectrum is practically identical in the four experiments. However, the use of different parametrizations when fitting the data, leads to same disagreements in the extracted a_1- parameters. Nevertheless, all results clearly indicate a lower mass and a substantially larger width for the a_1 resonance, than the ones obtained from hadronic experiments (PDG '86 values). More refined fits of the same data, including the q^2-dependence of the a_1-width which significantly shifts the value of the resonance-mass, have given the results shown in table 2.

Table 2

Reference	M_{a_1}(MeV)	Γ_{a_1}(MeV)
(15)	1235 ± 40	400 ± 100
(16)	1250 ± 40	600 ± 100
(17)	1260 ± 25	396 ± 43
(18)	1180 ± 50	450 ± 100
(19)	1220 ± 15	420 ± 40

Using the chiral information, the hadronic amplitude for the $\tau^- \to \nu_\tau \pi^+ \pi^- \pi^-$ decay takes the form ($q \equiv p_+ + p_-^1 + p_-^2$, $u \equiv (p_+ + p_-^1)^2$, $t \equiv (p_+ + p_-^2)^2$)

$$T_\mu(p_+,\ p_-^1,\ p_-^2) = \frac{2\sqrt{2}\,i}{3 f_\pi} F_{a_1}(q^2)\,(g_{\mu\nu} - q_\mu q_\nu/q^2)\Big[(p_+ - p_-^1)^\nu F_\rho(u) + (p_+ - p_-^2)^\nu F_\rho(t)\Big], \tag{2.7}$$

where the effect of the ρ and a_1 resonances has been already included. There are additional $J^P = 0^-$ contributions, but they are suppressed by a factor m_π^2/q^2 and therefore are completely negligible (notice that this implies $Br(\tau^- \to \pi^- \pi^o \pi^o) \simeq Br(\tau^- \to \pi^+ \pi^- \pi^-)$).

We can use this amplitude for making a fit to the three pion mass spectrum, taking $M_{a_1}^2$ and $\Gamma_{a_1} \equiv \Gamma_{a_1}(M_{a_1}^2)$ as free parameters. However, the normalization is completely fixed by the rigorous low-q^2 behaviour extracted from the chiral realization. Thus, once M_{a_1} and Γ_{a_1} have been fitted, eq. (2.7) gives us a non-trivial prediction for the branching ratio. Figure 2 compares the obtained q^2-distribution[20], taking $M_{a_1} = 1200$ MeV and $\Gamma_{a_1} = 475$ MeV, with the ARGUS data[12]. The result is surprisingly good; fitting the a_1-mass and width to agree

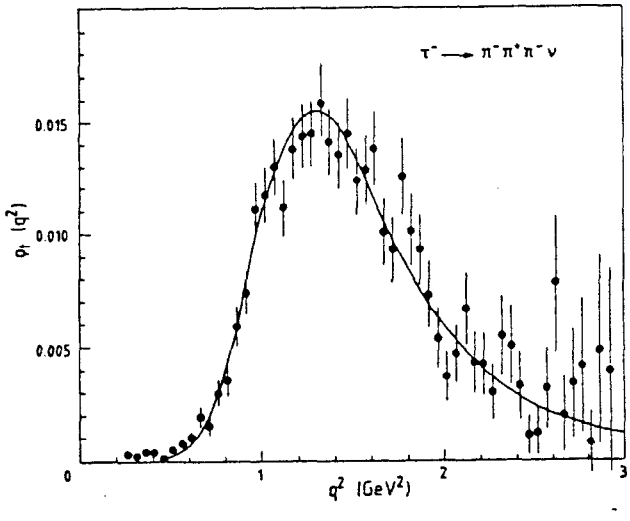

Fig. 2. Comparison between the measured[12] q^2-distribution for the $\tau^- \to \nu_\tau \pi^+ \pi^- \pi^-$ decay, and the theoretical result obtained from eq. (2.7), with $M_{a_1} = 1200$ MeV and $\Gamma_{a_1} = 475$ MeV. The normalization corresponds to $\rho_t(q^2) = 1/\pi \mathrm{Im}\Pi_A^{(1)}(q^2)$[12] (see eq. (3.2)).

with the shape of the invariant mass distribution, one finds that the normalization of the resulting curve is also in nice agreement with the experimental measurement. It is important to point out that, if one takes the old (86) particle data group values[14] for the resonance parameters, not only the shape of the predicted spectrum disagrees with the data but, in addition, the normalization at the maximum of the distribution is off by a factor of two.

The same approach has been applied to estimate the branching fractions for τ-decays with eta particles in the final state[9]. These modes where expected , two years ago, to provide some light on the so called missing one-prong problem[5a,21] (the sum of exclusive one-charged-particle modes is smaller than the measured inclusive branching fraction to one-charged-prong). Using the available information on the relevant resonances, one gets the results[9] shown in table 3, in order of increasing branching ratio.

Table 3

X^-	Br $(\tau^- \to \nu_\tau \eta x^-)$
$\pi^-\pi^o$	(0.2 - 0.3)%
K^-	10^{-4}
$\pi^-/\pi^-\bar{K}^o/K^-\pi^o$	10^{-5}
$\pi^-\pi^o\pi^o$	10^{-6}
K^-K^o	10^{-7}
$\pi^-\eta/K^-\eta$	10^{-9}

The inclusive production of η particles in τ decay is therefore dominated by the $\tau^- \to \nu_\tau \eta \pi^-\pi^o$ mode, with an expected[9,22] branching ratio of (0.2 - 0.3)%. This rules out a possible explanation of the missing one-prong branching fraction in terms of modes with η particles[23]. Nevertheless the decay into the final $\eta\pi^-\pi^o$ mode is interesting by itself. Due to the even G-parity of the η, this decay can only proceed through the vector current, which requires a vertex with a Levi-Civita antisymmetric tensor. The needed coupling is provided by the Wess-Zumino-Witten term of the chiral lagrangian, which gives rise to the odd-parity pieces in the currents given in eqs. (2.4). Therefore, the detection of the $\tau^- \to \nu_\tau \eta \pi^-\pi^o$ mode would constitute an experimental signal of the non-abelian chiral anomaly of QCD[9,24].

3. CURRENT CORRELATORS

It is convenient to consider the two point correlation functions

$$
\begin{aligned}
& i\int d^4x\, e^{iqx} \langle 0|T(V^\mu(x)_{ij}\, V^\nu(0)^+_{ij})|0\rangle \\
& \qquad \equiv (-g^{\mu\nu}q^2 + q^\mu q^\nu)\, \Pi_V^{(1)}(q^2)^{ij} + q^\mu q^\nu\, \Pi_V^{(0)}(q^2)^{ij} \\
& i\int d^4x\, e^{iqx} \langle 0|T(A^\mu(x)_{ij}\, A^\nu(0)^+_{ij})|0\rangle \\
& \qquad \equiv (-g^{\mu\nu}q^2 + q^\mu q^\nu)\, \Pi_A^{(1)}(q^2)^{ij} + q^\mu q^\nu\, \Pi_A^{(0)}(q^2)^{ij} \quad , \qquad (3.1)
\end{aligned}
$$

associated with the vector $V^\mu(x)_{ij} = \bar{q}_j \gamma^\mu q_i$ and axial $A^\mu(x)_{ij} = \bar{q}_j \gamma^\mu \gamma_5 q_i$ currents. Here i, j denote the quark flavours and the two different Lorentz structures in the r.h.s. correspond to J=1 and J=0 angular momentum. We can write down a spectral decomposition for these correlators

$$\Pi^{(1,0)}_{V,A}(q^2)^{ij} = \int_0^\infty ds \frac{\frac{1}{\pi} Im \Pi^{(1,0)}_{V,A}(s)^{ij}}{s - q^2 - i\varepsilon} + \text{substractions.} \qquad (3.2)$$

The associated spectral functions govern the $\tau \to \nu_\tau +$ hadrons decay width, which can be written as an integral over the invariant mass of the final hadrons[4],

$$R_H \equiv \frac{\Gamma(\tau^- \to \nu_\tau + \text{hadrons})}{\Gamma(\tau^- \to \nu_\tau e^- \bar{\nu}_e)} =$$

$$= 12\pi \int_0^{m_\tau^2} \frac{ds}{m_\tau^2} \left(1 - \frac{s}{m_\tau^2}\right)^2 \left\{ \left(1 + \frac{2s}{m_\tau^2}\right) Im \Pi^{(1)}(s) + Im \Pi^{(0)}(s) \right\}, \qquad (3.3)$$

where (r = 0, 1)

$$Im \Pi^{(r)}(s) \equiv \cos^2\vartheta_c \left\{ Im \Pi^{(r)}_V(s)^{12} + Im \Pi^{(r)}_A(s)^{12} \right\}$$

$$+ \sin^2\vartheta_c \left\{ Im \Pi^{(r)}_V(s)^{13} + Im \Pi^{(r)}_A(s)^{13} \right\}. \qquad (3.4)$$

In the chiral limit ($m_u = m_d = m_s = 0$), the longitudinal vector spectral functions vanish, while the corresponding axial ones have only the pole contribution from the Goldstone bosons, ($f \simeq f_\pi \simeq 93.3$ MeV)

$$\frac{1}{\pi} Im \Pi^{(0)}_V(s)^{12} = \frac{1}{\pi} Im \Pi^{(0)}_V(s)^{13} = 0$$

$$\frac{1}{\pi} Im \Pi^{(0)}_A(s)^{12} = \frac{1}{\pi} Im \Pi^{(0)}_A(s)^{13} = 2f^2\delta(s). \qquad (3.5)$$

In principle the vector and axial spectral functions are calculable in QCD, but in practice we are still very far away of being able to do that in the low energy region. The semileptonic tau decays offer the possibility to obtain experimentally these spectral functions, for s-values below m_τ^2, from the total invariant mass distribution of the final mesons. This analysis has been done by Peccei and Solá[25] in the Cabibbo allowed sector, where quite good data is already available. From a fit to the $\tau^\pm \to \nu_\tau \pi^\pm \pi^0$, $\tau^\pm \to \nu_\tau \pi^\pm \pi^+ \pi^-$ and $\tau^\pm \to \nu_\tau \pi^\pm \pi^+ \pi^- \pi^0$ s-distributions, measured by the ARGUS collaboration[12,26], and assuming the $\tau^\pm \to \nu_\tau \pi^\pm \pi^0 \pi^0$ contribution to be equal to the $\tau^\pm \to \nu_\tau \pi^\pm \pi^+ \pi^-$ one, they obtain the spectral functions shown in figure 3. Their notation corresponds to

$$v(s) \equiv 2\, Im \Pi^{(1)}_V(s)^{12} \; ; \; a(s) \equiv 2\, Im \Pi^{(1)}_A(s)^{12} \; . \qquad (3.6)$$

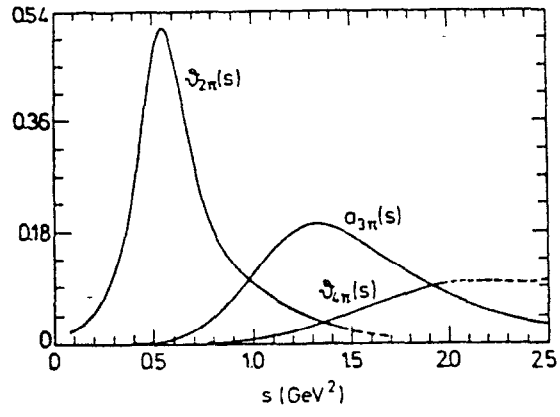

Fig. 3. The hadronic vector ($v = v_{2\pi} + v_{4\pi}$) and axial-vector ($a = a_{3\pi}$) spectral functions, extracted from semileptonic τ-decay data, as a function of s. The dashed lines denote the regions where the error bars start to be too big for the fit to be trustworthy. (Taken from ref. (25)).

The two and three pion contributions are clearly dominated by the ρ and a_1 peaks respectively, while the four pion contribution, which gives the bulk of the vector spectral function in the high s-region, doesn't show any prominent resonance structure. As one approaches the kinematical limit $s=m_\tau^2$, it becomes difficult to extract a reliable value for the spectral functions; thus the fit has rather large errors above $s=2\ GeV^2$.

We know from QCD that these spectral functions should have the asymptotic behaviour $a(s)=v(s)=1/2\pi = 0.159$. Therefore, large variations in both v(s) and a(s) are still to be expected at higher values of s. The axial spectral function, in particular, should substantially increase. Nevertheless, the experimental information summarized in figure 3 is good enough for testing some QCD expectations, at least qualitatively.

More than twenty years ago[27], Weinberg derived two sum rules for the vector and axial-vector spectral functions, using some general arguments related to the expected asymptotic behaviour of the strong interactions. In our notation, they read

$$\int_0^\infty ds \frac{1}{\pi} Im\left(\Pi_V^{(1)} + \Pi_V^{(0)} - \Pi_A^{(1)} - \Pi_A^{(0)}\right)(s)^{ij} = 0$$

$$\int_0^\infty ds\ s \frac{1}{\pi} Im\left(\Pi_V^{(1)} - \Pi_A^{(1)}\right)(s)^{ij} = 0. \qquad (3.7)$$

Although these sum rules were derived before the development of QCD, one can show[28] that they are actually approximately valid within QCD in the chiral limit. There are nowadays more refined versions of the Weinberg sum rules, which take into account the precise form of the leading short-distance behaviour of the current-correlators at large s-values and the explicit chiral symmetry breaking effects due to the finite quark masses[28,29]. However, since $m_{u,d} << m_\tau$ (3.7) are precise enough for analyzing the (i, j) = (1, 2) spectral functions.

Another classical sum rule, which makes use of these spectral functions, is the formula derived by Das et al. for the $\pi^{+-} - \pi^0$ electromagnetic mass difference[30]. In the chiral limit and making use of the second Weinberg sum rule, it can be written as

$$m_{\pi^+} - m_{\pi^0} = \frac{3\alpha}{16\pi\, m_\pi f_\pi^2} \int_0^\infty ds\, s\, \frac{1}{\pi}\, Im\left(\Pi_A^{(1)} - \Pi_V^{(1)}\right)(s)\, {}^{12}\ln s \qquad (3.8)$$

Assuming that the spectral functions are saturated by the ρ and a_1 mesons and using the KSFR relation, Das et al obtained[30]

$$m_{\pi^+} - m_{\pi^0} \simeq \frac{3\alpha}{4\pi} \frac{M_\rho^2}{m_\pi} \ln 2 \simeq 5 \text{ MeV}, \qquad (3.9)$$

in amazing agreement with the experimental value[1] of 4.6 MeV.

Eqs. (3.7) and (3.8) involve integrations of the relevant spectral functions from zero to infinity. However, the asymptotic behaviour predicted by QCD implies that the contributions of the very high s-region are completely negligible. Therefore, it is interesting to see how well one does when one integrates up to a maximum limit so. Using the spectral functions shown in figure 3, Peccei and Solá have studied the integrals[25]

$$I_1(so) = \int_0^{so} ds\, (v(s) - a(s))$$

$$I_2(so) = \int_0^{so} ds\, s\, (v(s) - a(s))$$

$$\Delta(\pi^+ - \pi^0) = \frac{3\alpha}{32\pi^2\, m_\pi f_\pi^2} \int_0^{so} ds\, s\, \ln s\, (a(s) - v(s)). \qquad (3.10)$$

Their results are plotted in figures 4, as function of the integration cut off so. The crosshatched area represents the region in which the determination of the spectral functions is less certain. Remarkably, all three quantities approach the closest to the predicted asymptotic values ($4\pi f_\pi^2 = 0.11$ GeV^2, 0 , and 4.6 MeV, respectively) at the same so = 2 GeV^2 value. This suggests in fact that the vector and axial-vector spectral function contributions cancel each other already at quite moderate values of s. It is for this reason that the resonance saturation formula (3.9) works so well. Note however that using the exact form of $v_{2\pi}$ and $a_{3\pi}$ extracted from the semileptonic tau-decay data, the contribution of $v_{4\pi}$ is rather important. Neglecting this term, one would obtain[25] $\Delta(\pi^+ - \pi^0) = 7$ MeV at so = 2 GeV^2, rather than about 4.6 MeV. It is also clear from the figures, that to recover the expected QCD predictions it is ne- cessary that eventually, for some higher region of s, a(s)>v(s), to compensate the wrong behaviour observed in the so-range between 2 and 2.5 GeV^2. That was already apparent in figure 3, because at s = 2.5 GeV^2 a(s) is much smaller than v(s).

By making a Laplace transform of eqs. (3.7)[29] one can exponentially suppress the contribution of high values of s to the Weinberg sum rules. The truncated integrals are then[25], for moderate values of the Laplace parameter ($K^2 \sim 1 - 1.5$ GeV^2), essentially independent on whether one cuts off them at s_o = 2 GeV^2 or s_o = 2.5 GeV^2. The Laplace transform version of the first Weinberg sum rule appears to be in good agreement with the asymptotic QCD prediction[25]. It remains, however, a larger discrepancy for the case of the second sum rule,

which can be understood since the additional power of s makes the exponential suppression less effective and therefore the contribution of the tail integral ($s > s_o$) is not negligible in this case[25].

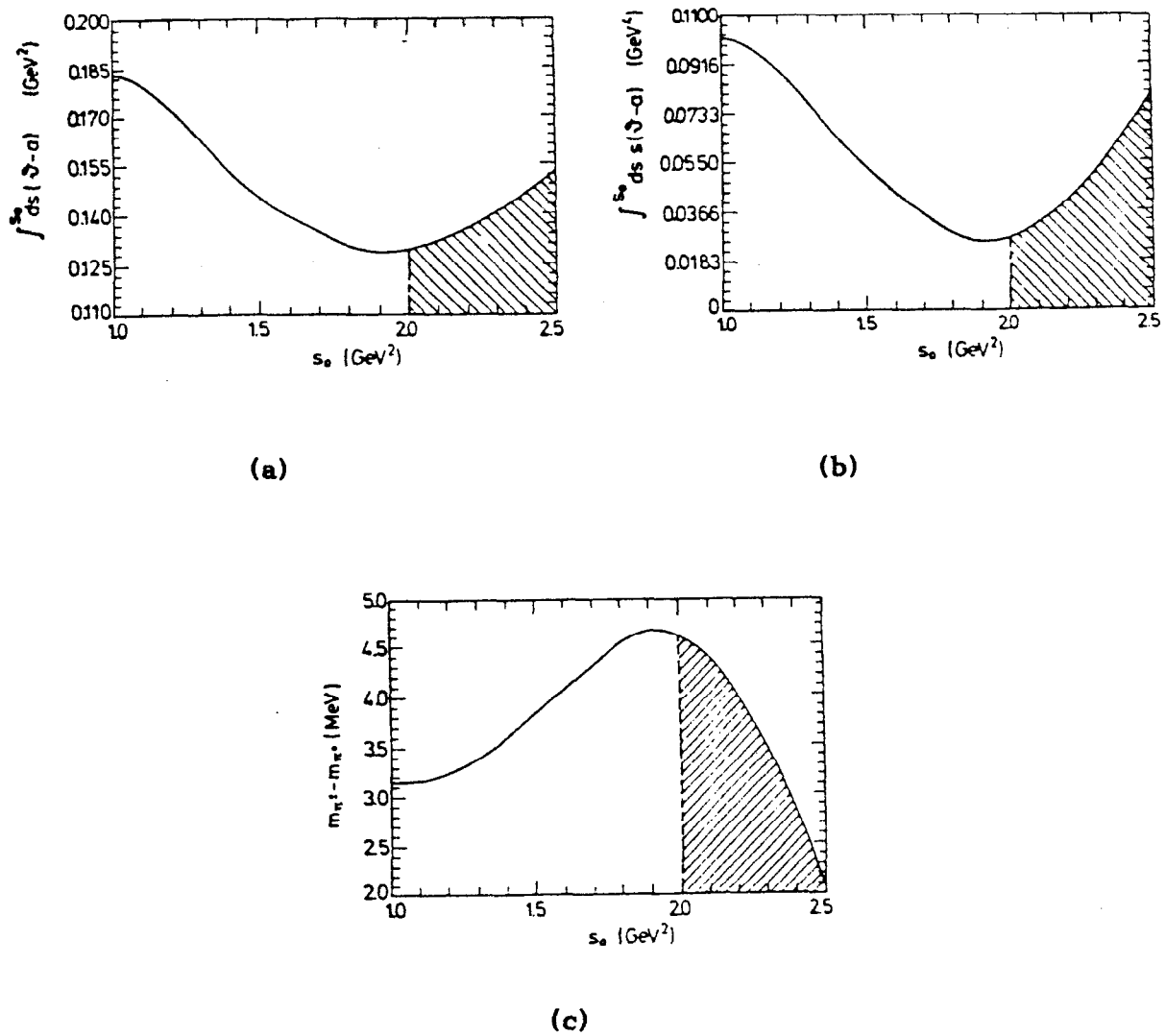

Fig. 4. Behaviour of the 1st (a) and 2nd (b) Weinberg sum rules and the electromagnetic pion mass difference (c), as a function of the upper limit of integration s_o. The dashed areas use $v_{4\pi}$ in the questionable region of figure 3. (Taken from ref. (25)).

4. VACUUM CONDENSATES

At high values of q^2 one can use perturbative QCD to evaluate the two point correlators defined in eq. (3.1). Moreover, non-perturbative effects, which are parametrized by a set of vacuum expectation values of quark and gluon fields, can be included as power corrections to asymptotic freedom[31]. For the $J^P = 1^-$, (i, j) = (1, 2) correlator, one gets[31,32] ($Q^2 \equiv -q^2$)

$$4\pi^2 \Pi_V^{(1)}(Q^2)^{12} = -\ln\frac{Q^2}{\nu^2} + \frac{5}{3} + O(m^2_{u,d}/Q^2)$$

$$-\frac{\alpha_s(\nu^2)}{\pi} \ln\frac{Q^2}{\nu^2} + O\left((\alpha_s/\pi)^2\right)$$

$$+\sum_{n=2} \frac{C_{2n}\langle O_{2n}\rangle_\nu}{(Q^2)^n} , \qquad (4.1)$$

where the leading non-perturbative correction is given, in the $m_u = m_d = \hat{m}$ limit, by[31]

$$C_4\langle O_4\rangle_V = \frac{\pi}{3}\langle\alpha_s G^2\rangle + 4\pi^2 \hat{m}\langle\bar{u}u + \bar{d}d\rangle \qquad (4.2)$$

Due to the conservation of the vector current, $\Pi_V^{(0)}(q^2)^{12}$ is zero in the i-sospin limit. For the axial two-point function, the Goldstone nature of the pion makes difficult to separate the 0^- and 1^+ correlators, so it is better to work with the sum

$$\Pi_A(q^2)^{12} \equiv \Pi_A^{(1)}(q^2)^{12} + \Pi_A^{(0)}(q^2)^{12}. \qquad (4.3)$$

The perturbative QCD expression for $\Pi_A(q^2)^{12}$ is the same as that for $\Pi_V(q^2)^{12}$, except for small quark-mass corrections. The leading non-perturbative term is given by[31]

$$C_4\langle O_4\rangle_A = \frac{\pi}{3}\langle\alpha_s G^2\rangle - 4\pi^2 \hat{m}\langle\bar{u}u + \bar{d}d\rangle. \qquad (4.4)$$

Note that the difference between the dimension four non-perturbative terms in the axial and vector correlators, can be estimated through PCAC,

$$C_4\langle O_4\rangle_A - C_4\langle O_4\rangle_V = -8\pi^2 \hat{m}\langle\bar{u}u+\bar{d}d\rangle$$

$$= 8\pi^2 f_\pi^2 m_\pi^2 \simeq 0.013\ \text{GeV}^4 \quad . \qquad (4.5)$$

Information on these non-perturbative power corrections can be obtained experimentally, by using Finite Energy Sum Rules (FESR) in the way derived in reference (33):

$$C_{4N+2}\langle O_{4N+2}\rangle_{V,A} = 4\pi^2 \int_0^{s_0} ds\, s^{2N} \frac{1}{\pi} \mathrm{Im}\Pi_{V,A}(s)^{12}$$

$$- \frac{s_0^{2N+1}}{2N+1} \left[1 + F_{4N+2}(s_0)\right]$$

(4.6)

$$C_{4N+4}\langle O_{4N+4}\rangle_{V,A} = -4\pi^2 \int_0^{s_0} ds\, s^{2N+1} \frac{1}{\pi} \mathrm{Im}\Pi_{V,A}(s)^{12}$$

$$+ \frac{s_0^{2N+2}}{2N+2} \left[1 + F_{4N+4}(s_0)\right]$$

Here, $N = 0, 1, 2, \ldots$, and the functions $F_p(s_0)$, with $p = 4N+2$ or $p = 4N+4$, contain the perturbative α_s-corrections. Selecting the appropriate moment of the spectral function distribution, eqs. (4.6) project a specific combination of vacuum expectation values of operators of a given dimension*).

The l.h.s. of eqs. (4.6) are obviously independent of the chosen value for the asymptotic freedom onset s_0. In practice, the r.h.s. will give a so-dependence either if s_0 is not high enough for the perturbative calculation contained in $F_p(s_0)$ to be reliable, or if the hadronic information contained in the spectral function is not good enough in the whole $s<s_0$ region. The predictions from the FESR should only be trusted provided they are stable against reasonable changes of s_0 inside some duality region, where both informations (QCD and hadronic) are simultaneously valid[34]. This duality region can be determined by using the lowest moment N=0. Since the $\hat{m}^2/Q^2$ corrections to the two-point correlators, formally equivalent to a $C_2\langle O_2\rangle$ effective contribution, are negligible, one has

$$1 + F_2(s_0) = I_0(s_0)_{V,A} \equiv \frac{4\pi^2}{s_0} \int_0^{s_0} ds\, \frac{1}{\pi} \mathrm{Im}\, \Pi_{V,A}(s)^{12}, \qquad (4.7)$$

which gives an eigenvalue equation to fix the parameter s_0. The more accurate the parametrization of the experimental data is, the wider the duality s_0-region, solution of the above equation, will be. Once s_0 is determined, one may proceed to estimate the values of $C_p\langle O_p\rangle$ using eqs. (4.6).

Figures 5 to 8 show the results obtained in reference (35), using the hadronic spectral functions extracted from the semileptonic τ-decay data[25]. The duality test of eq. (4.7) is plotted in figures 5 and 7 for the vector and axial vector spectral functions respectively. Curve (a) corresponds to the behaviour of the hadronic integral in the r.h.s. of the FESR (4.7), while curve (b) gives the smooth s_0-dependence given by the QCD l.h.s. In the vector channel one finds a duality region inthe range $1.44\ \mathrm{GeV}^2 \leq s_0 \leq 1.75\ \mathrm{GeV}^2$, while for the axial-vector channel the duality region is somewhat wider, $1.75\ \mathrm{GeV}^2 \leq s_0 \leq 2.25\ \mathrm{GeV}^2$.

*) This nice feature disappears when two-loop corrections to the Wilson coefficients C_p are taken into account.

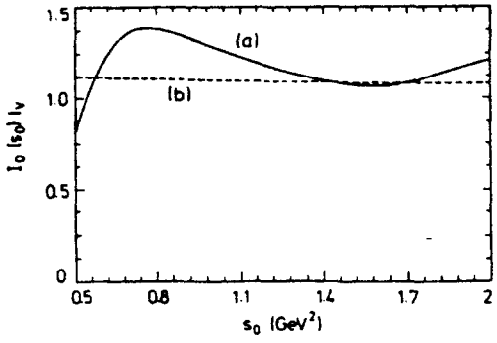

Fig.5. Behaviour of the hadronic integral in the r.h.s. of the FESR (4.7) (curve a) together with the behaviour of the QCD l.h.s. (curve b) in the vector channel. (Taken from ref. (35)).

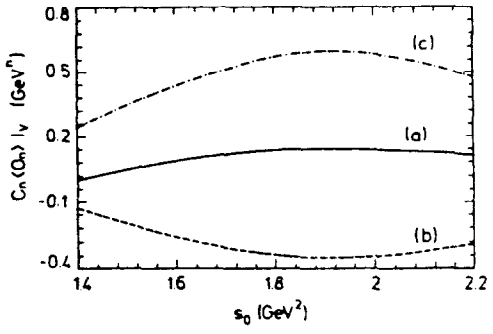

Fig. 6. Behaviour of $C_p\langle O_p\rangle_V$ for p = 4 (curve a), 6 (curve b) and 8 (curve c), from the FESR (4.6). (Taken from ref. (35)).

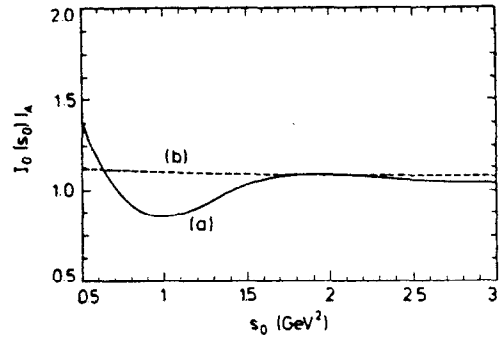

Fig. 7. Same as fig. 5 in the axial-vector channel.

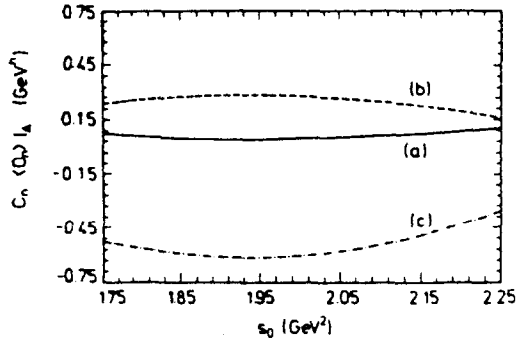

Fig. 8. Same as fig. 6 in the axial-vector channel.

Solving next the FESR (4.6) for values of s_0 inside these regions one finds the results shown in figure 6 for the vector channel and in figure 8 for the axial-vector one[35]. Curves (a), (b) and (c), correspond here to $C_4\langle O_4\rangle_{V,A}$, $C_6\langle O_6\rangle_{V,A}$ and $C_8\langle O_8\rangle_{V,A}$ respectively. The vacuum condensates turn out to be reasonably stable against changes within the duality region. Note that the axial-vector results are more stable, and therefore less inaccurate, than the ones obtained in the vector channel. Numerically the results are

$$C_4\langle O_4\rangle_V = (0.025 - 0.11)\ \text{GeV}^4 \quad ; \quad C_4\langle O_4\rangle_A = (0.045 - 0.10)\ \text{GeV}^4$$
$$C_6\langle O_6\rangle_V = -(0.16 - 0.32)\ \text{GeV}^6 \quad ; \quad C_6\langle O_6\rangle_A = (0.16 - 0.28)\ \text{GeV}^6$$
$$C_8\langle O_8\rangle_V = (0.28 - 0.55)\ \text{GeV}^8 \quad ; \quad C_8\langle O_8\rangle_A = -(0.36 - 0.54)\ \text{GeV}^8. \qquad (4.8)$$

Eqs. (4.2), (4.4) and (4.5) allow to extract the value of the gluon condensate both from $C_4\langle O_4\rangle_V$ and $C_4\langle O_4\rangle_A$,

$$\frac{\pi}{3}\langle\alpha_s G^2\rangle = \begin{cases} (0.03 - 0.12)\ \text{GeV}^4, \text{ (vector channel)} \\ (0.04 - 0.09)\ \text{GeV}^4, \text{ (axial-vector channel)} \end{cases} . \qquad (4.9)$$

It is rewarding that the use of two independent sets of experimental data lead to essentially the same value for the gluon condensate. This result is consistent with the ones obtained using experimental information on charmonium or e^+e^- cross sections[36].

The values found for the dimension d = 6 four-quark condensates $C_6\langle O_6\rangle_{V,A}$ indicate, in agreement with earlier claims, a clear deviation from the standard vacuumm saturation approximation, which predicts[31] $C_6\langle O_6\rangle_V \sim -(7/11)\ C_6\langle O_6\rangle_A \sim -0.06\ \text{GeV}^6$. On the other side, the rather large values obtained for the dimension d= 8 condensates and the clear sign difference between $C_8\langle O_8\rangle_V$ and $C_8\langle O_8\rangle_A$ could have important theoretical consequences. This condensates are usually assumed[37] to be dominated by four-gluon operators, which should give the same contribution to the vector and axial-vector channels. This suggest that other contributions apart from gluons could be relevant.

The values of the vacuum condensates can also be extracted by using Laplace transform sum rules[31]. Because of its exponential weight, the Laplace transform places more emphasis on the low energy part of the hadronic spectral function, which is a clear advantage. However, now all of the condensates appear in the same sum rule, in contrast with the FESR where vacuum condensates of different dimensionality obey uncoupled equations. Although higher dimensional condensates become factorially suppressed by the Laplace transform, this may be not enough to safely neglect them when trying to determine the condensates of lowest dimension. In practice, one needs to truncate the $1/Q^2$ power series in eq. (4.1) keeping only a finite number of terms. This introduces an unavoidable bias in the sense that the values obtained for the condensates will depend on how many terms of the series have been taken into account. Using the axial spectral function extracted[25] from semileptonic tau decay data, this dependence has been analyzed in reference (38), where it is shown that, although the results change substantially with N when only a small number N of terms are included, the procedure is convergent with increasing N. The obtained results[38]

$$\frac{C_4\langle O_4\rangle_A}{C_6\langle O_6\rangle_A} = (0.28 \pm 0.01 \pm 0.05)\ \text{GeV}^{-2}$$

$$\frac{C_6\langle O_6\rangle_A}{C_8\langle O_8\rangle_A} = -(0.51 \pm 0.03 \pm 0.08)\ \text{GeV}^{-2} \qquad (4.10)$$

are in agreement with the determination[35] with FESR.

The results (4.8) and (4.10) have been derived using the computed perturbative contributions to the $\Pi_{V,A}(q^2)$ correlators up to third order terms. The α_s^3-correction to these two-point functions has been calculated recently and it has been found to be rather large[39]. It would be interesting to analyze how much the condensate values change when this higher order correction is included.

5. DETERMINATION OF $\Lambda_{\overline{MS}}$

We have already seen in eq. (3.3) that the semileptonic decay width of the tau lepton is governed by an integral, over the invariant mass of the final hadrons, of the vector and axial-vector spectral functions. In fact, eq. (3.3) is just a combination of different moments of the spectral functions of the type appearing in the FESR (4.6), with $s_0 = m_\tau^2$. Only the moments s^0, s^2 and s^3 appear in the dominant J = 1 channels; therefore, the semileptonic tau decay width will only get non-perturbative contributions from condensates of dimension 6 and 8[40]. Including[40] the four-loop calculation of reference (39), the ratio R_H is given, in the $\overline{MS}$-scheme, by[40,41]

$$R_H = 3\, r_H \left\{ 1 + \frac{\alpha_s(m_\tau)}{\pi} + 5.20 \left(\frac{\alpha_s(m_\tau)}{\pi}\right)^2 + 104.0 \left(\frac{\alpha_s(m_\tau)}{\pi}\right)^3 + \ldots \right.$$
$$\left. + \frac{C_2 \langle O_2 \rangle_{V+A}}{m_\tau^2} - 3\,\frac{C_6 \langle O_6 \rangle_{V+A}}{m_\tau^6} - 2\,\frac{C_8 \langle O_8 \rangle_{V+A}}{m_\tau^8} \right\}, \tag{5.1}$$

where[2] $r_H = 1.0215 \pm 0.0050$ is the estimated electroweak correction (including the $|V_{ud}|^2 + |V_{us}|^2 \simeq 0.9979$ mixing factor), and $C_2\langle O_2\rangle_{V+A}$ stands for the small perturbative quark mass effects[40].

Since the leading non-perturbative condensates of dimension four doesn't contribute to R_H, non-perturbative effects are suppressed by additional powers of the tau mass. Moreover, as shown in eqs. (4.8), there is a strong cancellation between the vector and axial-vector contributions to the dimension six and eight condensates. Taking also into account information on the vacuum condensates coming from other sources[36], the total effect of non-perturbative contributions to R_H was estimated in reference (40) to be in the range -0.6% to -1/3%.

The most important corrections are due to the radiative gluonic contributions, which are of positive sign as needed to reproduce the experimental value of R_H. The large coefficient of the α_s^3-term is, however, rather uncomfortable, since it can cast some doubts on the meaning of the perturbative QCD-calculation. The question is to know what is going to happen with the uncalculated next-order contributions. Note, that this problem has nothing to do with the tau mass scale; it is the α_s^3-correction to the vector and axial-vector spectral functions, which happens to have a large coefficient. Therefore, the same comments apply to the QCD-prediction for the total e^+e^- hadronic cross section at higher energies. On the other side, this large α_s^3-contribution makes the predicted value of R_H strongly dependent on the QCD scale $\Lambda_{\overline{MS}}$. One could then use the semileptonic tau decay to obtain a determination of $\Lambda_{\overline{MS}}$[40]. Varying $\Lambda_{\overline{MS}}$ (defined in the 3-flavour theory) from 100 to 300 MeV, one gets the results shown in table 4. In order to have a feeling on the possible error due to the uncalculated higher order perturbative corrections, I have computed R_H in two different ways. The values shown in column (a), have been obtained[40] expanding the strong coupling constant $\alpha_s(m_\tau)$ in powers of $a_s \equiv -1/\beta_1 \ln(m_\tau/\Lambda_{\overline{MS}})$, and keeping the contributions to R_H up to order a_s^4. In column (b), the complete three-loop calculation of $\alpha_s(m_\tau)$ has been used to eva-

luate the different terms appearing in eq. (5.1). The quoted errors are an estimate of the small uncertainties associated with the non-perturbative contributions.

Table 4

$\Lambda_{\overline{MS}}$ (MeV)	R_H (a)	R_H (b)
100	3.40 ± 0.01	3.34 ± 0.01
200	3.67 ± 0.01	3.51 ± 0.01
300	4.03 ± 0.01	3.71 ± 0.01

The differences between the two columns clearly indicate that the uncertainty of the theoretical predictions is completely dominated by the effect of the large α_s^3-correction, and grows for increasing values of $\Lambda_{\overline{MS}}$.

The ratio R_H is related to the total tau-decay width through the equation

$$\Gamma(\tau^-) = \Gamma(\tau^- \longrightarrow \nu_\tau e^- \bar{\nu}_e) \left\{ 1.9728 + R_H \right\} . \qquad (5.2)$$

S_O, R_H can be obtained experimentally either from the leptonic branching ratios, or from the lifetime measurement, if the theoretical prediction (1.4) for the leptonic width is assumed. One finds

$$R_H \Big|_{exp} = \begin{cases} 3.74 \pm 0.13 & , \quad \text{from } Br(\tau^- \longrightarrow \nu_\tau e^- \bar{\nu}_e) \\ 3.49 \pm 0.12 & , \quad \text{from } Br(\tau^- \longrightarrow \nu_\tau \mu^- \bar{\nu}_\mu) \\ 3.29 \pm 0.17 & , \quad \text{from lifetime} \end{cases} , \qquad (5.3)$$

which shows another time the discrepancy between the lifetime and leptonic branching ratios measurements, mentioned in section 1. One can also estimate R_H by directly summing the measured exclusive widths of the different hadronic channels; this gives a smaller value[40], $R_H = 3.22 \pm 0.10$, reflecting the well known missing one-prong problem. If one does a formal average[2] of the three R_H-values in eq. (5.3), one gets

$$R_H \Big|_{exp.} = 3.54 \pm 0.08 \ , \qquad (5.4)$$

which seems to favour a value of $\Lambda_{\overline{MS}}$ around 200 MeV. Given the present experimental discrepancies, however, we can anly conclude[40] that the lifetime and exclusive decays measurements require $\Lambda_{\overline{MS}} \sim 100$ MeV, while higher values for the QCD scale are preferred by the experimental leptonic branching ratios. Future high precision experiments will certainly clarify the present disagreements among different measurements, allowing for a more accurate determination of $\Lambda_{\overline{MS}}$. In this respect, it would be useful to get a better understanding of the large α_s^3-correction appearing in the vector an axial-vector

spectral functions. Since the same perturbative QCD-calculation can be tested with two different experimental measurements, hadronic tau-decay width and $e^+e^- \rightarrow$ hadrons cross-section, the comparison of the results obtained from the two experiments, including the α_s^3-term, will provide some light on the phenomenological role of this large higher-order contribution. At present, the $\Lambda_{\overline{MS}}$-values extracted from both experimental measurements do, in fact, agree.

6. SUMMARY

The semileptonic tau-decay data is an ideal laboratory for studying the algebra of currents of QCD. Information on both vector and axial-vector currents can be obtained in a very clean experimental environment. The invariant mass distribution of the final hadrons, in addition to provide clear signals of resonance structures, allows to test different aspects of strong interaction phenomena (non-abelian chiral-anomaly, Weinberg sum rules, pion mass difference, ...), which are related to the global chiral symmetry properties of QCD. Information on the structure of the QCD-vacuum is directly obtained from appropriate weighted integrations of the hadronic spectrum. Perturbative QCD predictions can also be compared with the measured total hadronic tau-decay width, to infer a value for the QCD-scale $\Lambda_{\overline{MS}}$. Therefore, accurate experimental information on the decay modes of the tau, coming from future high-luminosity machines, will become an extremely useful tool for our understanding of the strong interactions.

ACKNOWLEDGEMENTS

I would like to thank the organizers for the charming atmosphere of this workshop. This work has been partly supported by C.I.C.Y.T., Spain, under grant No. AEN88-0021.

REFERENCES

1. M. Aguilar-Benitez et al., Review of Particle Properties, Phys. Lett. B204 (1988) 1.

2. W.J. Marciano and A. Sirlin, Phys. Rev. Lett. 61 (1988) 1815.

3. H. Albrecht et al. (ARGUS), Phys. Lett. B202 (1988) 149.

4. Y.-S. Tsai, Phys. Rev. D9 (1971) 2821.

5. F.J. Gilman and S.H. Rhie, Phys. Rev. D31 (1985) 1066.
F.J. Gilman and D.H. Miller, Phys. Rev. D17 (1978) 1846.

6. A good introduction to chiral lagrangians is given in H. Georgi, "Weak Interactions and Modern Particle Theory", Benjamin/Cummings Publish. Comp. Inc. (Menlo Park, California) 1984.

7. J. Wess and B. Zumino, Phys. Lett. B37 (1971) 95.
E. Witten, Nucl. Phys. B223 (1983) 422.

8. R. Fischer, J. Wess and F. Wagner, Z. Phys. C3 (1980) 313.

9. A. Pich, Phys. Lett. B196 (1987) 561.

10. W. Ruckstuhl et al. (DELCO), Phys. Rev. Lett. 56 (1986) 2132.

11. W.B. Schmidke et al. (MARK II), Phys. Rev. Lett. 57 (1986) 527.

12. H. Albrecht et al. (ARGUS), Z. Phys. C33 (1986) 7.

13. H.R. Band et al. (MAC), Phys. Lett. B198 (1987) 297.

14. M. Aguilar-Benitez et al., Review of Particle Properties, Phys. Lett. B170 (1986) 1.

15. M.G. Bowler, Phys. Lett. B182 (1986) 400.

16. N.A. Tornquist, Z. Phys. C36 (1987) 695.

17. M.G. Bowler, preprint Oxford Univ. (1988)

18. T. Berger, Z. Phys. C37 (1987) 95.

19. N. Isgur, C. Morningstar and C. Reader, Phys. Rev. D39 (1989) 1357.

20. A. Pich, unpublished work 1987.

21. T.N. Truong, Phys. Rev. D30 (1984) 1509.

22. F.J. Gilman, Phys. Rev. D35 (1987) 3541.

23. A. Pich, Proc. of the International Euro physics Conference on High Energy Physics (Uppsala, Sweden, 1987), ed. O. Batner, Uppsala University 1987, 339.

24. G. Kramer and W.F. Palmer, Z. Phys. C25 (1984) 195.

25. R.D.Peccei and J. Solá, Nucl. Phys. B281 (1987) 1.

26. A. Golutvin and U. Binder, private communication quoted in ref. (25).

27. S. Weinberg, Phys. Rev. Lett. 18 (1967) 507.

28. E. Floratos, S. Narison and E. de Rafael, Nucl. Phys. B155 (1979) 115.

29. P.Pascual and E. de Rafael, Z. Phys. C12 (1982) 127.
S. Narison, Z. Phys. C14 (1982) 263.

30. T. Das et al., Phys. Rev. Lett. 19 (1967) 759.

31. M.A. Shifman, A.I. Vainshtein and V.I. Zakharov, Nucl. Phys. B147 (1979) 385.

32. E. de Rafael, Proc. of the X GIFT International Seminar on Theoretical Physics (Jaca, Spain, 1979), eds. J.L. Alonso and R. Tarrach, Lecture Notes in Physics No. 118, Springer (Berlin 1980), p. 1.

33. R.A. Bertlmann, G. Launer and E. de Rafael, Nucl. Phys. B250 (1985) 61.

34. A. Pich and E. de Rafael, Phys. Lett. B158 (1985) 477.

35. C. A. Dominguez and J. Solà, Z. Phys. C40 (1988) 63.

36. R.A. Bertlmann et al., Z. Phys. C39 (1988) 231, and references therein.

37. D.J. Broadhurst and S.C. Generalis, Phys. Lett. B165 (1985) 175.

38. V. Gimenez, J.A. Peñarrocha and J. Bordes, Phys. Lett. B223 (1989) 221.

39. S.G. Gorishny, A.L. Kataev and S.A. Larin, Phys. Lett. B212 (1988) 238.

40. A. Pich and S. Narison, Phys. Lett. B211 (1988) 183.

41. E. Braaten, Phys. Rev. Lett. 60 (1988) 1606; Phys. Rev. D39 (1989) 1458.